Journal of Physiology (2002), **540.1**, *pp.* 105–117
DOI: 10.1113/jphysiol.2001.013184

www.jphysiol.org

Ca^{2+}-activated Cl^- current in rabbit sinoatrial node cells

Arie O. Verkerk*, Ronald Wilders*†, Jan G. Zegers*, Marcel M. G. J. van Borren*, Jan H. Ravesloot* and E. Etienne Verheijck*

*Academic Medical Center, University of Amsterdam, Task Force Heart Failure and Aging, Department of Physiology, Meibergdreef 15, 1105 AZ Amsterdam and †University Medical Center Utrecht, Department of Medical Physiology, Utrecht, The Netherlands

The Ca^{2+}-activated Cl^- current ($I_{Cl(Ca)}$) has been identified in atrial, Purkinje and ventricular cells, where it plays a substantial role in phase-1 repolarization and delayed after-depolarizations. In sinoatrial (SA) node cells, however, the presence and functional role of $I_{Cl(Ca)}$ is unknown. In the present study we address this issue using perforated patch-clamp methodology and computer simulations. Single SA node cells were enzymatically isolated from rabbit hearts. $I_{Cl(Ca)}$ was measured, using the perforated patch-clamp technique, as the current sensitive to the anion blocker 4,4′-diisothiocyanostilbene-2,2′-disulphonic acid (DIDS). Voltage clamp experiments demonstrate the presence of $I_{Cl(Ca)}$ in one third of the spontaneously active SA node cells. The current was transient outward with a bell-shaped current–voltage relationship. Adrenoceptor stimulation with 1 μM noradrenaline doubled the $I_{Cl(Ca)}$ density. Action potential clamp measurements demonstrate that $I_{Cl(Ca)}$ is activate late during the action potential upstroke. Current clamp experiments show, both in the absence and presence of 1 μM noradrenaline, that blockade of $I_{Cl(Ca)}$ increases the action potential overshoot and duration, measured at 20 % repolarization. However, intrinsic interbeat interval, upstroke velocity, diastolic depolarization rate and the action potential duration measured at 50 and 90 % repolarization were not affected. Our experimental data are supported by computer simulations, which additionally demonstrate that $I_{Cl(Ca)}$ has a limited role in pacemaker synchronization or action potential conduction. In conclusion, $I_{Cl(Ca)}$ is present in one third of SA node cells and is activated during the pacemaker cycle. However, $I_{Cl(Ca)}$ does not modulate intrinsic interbeat interval, pacemaker synchronization or action potential conduction.

(Received 24 August 2001; accepted after revision 20 December 2001)
Corresponding author A. Verkerk: Academic Medical Center, Department of Physiology, Room M01-09, Meibergdreef 15, 1105 AZ Amsterdam, The Netherlands. Email: A.O.Verkerk@amc.uva.nl

Atrial, Purkinje and ventricular myocytes from different species have been demonstrated to express a Ca^{2+}-activated Cl^- current ($I_{Cl(Ca)}$) (for reviews, see Sorota, 1999; Hume *et al.* 2000). $I_{Cl(Ca)}$ is the 4-aminopyridine insensitive part of the transient outward current and is also termed I_{to2}. $I_{Cl(Ca)}$ is primarily activated by Ca^{2+} ions released from the sarcoplasmic reticulum (Sipido *et al.* 1993; Kawano *et al.* 1995). The current does not follow the time course of the intracellular Ca^{2+} transients, but reaches a peak within 10–20 ms and then inactivates in the following 100 ms (Zygmunt & Gibbons, 1991, 1992; Sipido *et al.* 1993). It is postulated that this transient behaviour may be due to an intrinsic Ca^{2+}-dependent inactivation of $I_{Cl(Ca)}$ or may be due to the time course of local, subsarcolemmal Ca^{2+} gradients (Sipido *et al.* 1993; Zygmunt, 1994; Kawano *et al.* 1995).

The reversal potential for Cl^- ions (E_{Cl}) in cardiomyocytes is approximately −50 mV (Sorota, 1999). Therefore, activation of $I_{Cl(Ca)}$ has the potential, in theory, to generate an inwardly directed, depolarizing current at resting membrane potentials, whereas it generates an outwardly directed, repolarizing current during phase-1 and phase-2 of the action potential. Indeed, it has been demonstrated experimentally that $I_{Cl(Ca)}$ strongly influences phase-1 repolarization of atrial (Wang *et al.* 1995) and ventricular action potentials (Hiraoka & Kawano, 1989; Kawano & Hiraoka, 1991), especially under conditions of adrenoceptor stimulation (Verkerk *et al.* 2001). Moreover, it has been demonstrated that $I_{Cl(Ca)}$ contributes to the potentially arrhythmogenic delayed after-depolarizations in Purkinje and ventricular cells (Zygmunt *et al.* 1998; Verkerk *et al.* 2000). These findings indicate that $I_{Cl(Ca)}$ plays a substantial role in atrial, Purkinje and ventricular electrophysiology.

The presence of $I_{Cl(Ca)}$ in sinoatrial (SA) node cells is unknown. In SA node tissue, the sarcoplasmic reticulum is relatively sparse compared with atrial cells (Masson-Pévet *et al.* 1978). Nevertheless, cultured and freshly isolated mammalian SA node cells show clear intracellular Ca^{2+} transients (Li *et al.* 1997; Huser *et al.* 2000; Rigg *et al.* 2000; Bogdanov *et al.* 2001) as do amphibian pacemaker cells (Ju & Allen, 1999, 2000), indicating that the substrate for activating $I_{Cl(Ca)}$ in SA node cells is present. The present

study was designed to assess the presence and functional role of $I_{Cl(Ca)}$ in single SA node cells of rabbit. We report that $I_{Cl(Ca)}$ is present in one third of the rabbit SA node cells. Action potential clamp measurements show that $I_{Cl(Ca)}$ is activated during the normal pacemaker cycle late during the action potential upstroke. Blockade of $I_{Cl(Ca)}$ results in an increase of the action potential overshoot. Noradrenaline (1 μM) doubled the size of $I_{Cl(Ca)}$, but even under such conditions, $I_{Cl(Ca)}$ did not change the firing rate. We incorporated $I_{Cl(Ca)}$ into our previously published model of a rabbit SA node cell (Wilders *et al.* 1991), and used this model to assess the functional role of $I_{Cl(Ca)}$ in pacemaker activity. The computer simulations show that $I_{Cl(Ca)}$ has minimal effects on synchronization of SA nodal cells and action potential conduction between SA nodal and atrial cells.

METHODS

Cell preparation

All experiments were carried out in accordance with guidelines of the local Institutional Animal Care and Use Committee. Single SA node cells were isolated from rabbit hearts by an enzymatic dissociation procedure as described by Verheijck *et al.* (1995). The hearts were obtained from New Zealand White rabbits (body weight: 3.0–3.5 kg), which were anaesthetized with a 1 ml kg^{-1} intramuscular injection of Hypnorm (10 mg ml^{-1} fluanisone and 0.315 mg ml^{-1} fentanyl citrate; Jansen Pharmaceutics, Tilburg, The Netherlands). Small aliquots of cell suspension were put in a recording chamber on the stage of an inverted microscope. Cells were allowed to adhere for 5 min after which perfusion with Tyrode solution (36 ± 0.5 °C) was started. The Tyrode solution contained (mM): NaCl 140, KCl 5.4, $CaCl_2$ 1.8, $MgCl_2$ 1.0, glucose 5.5 and Hepes 5.0 (pH was adjusted to 7.4 with NaOH). Cells were dissociated from the entire SA node region and represent a mixed population of cells showing heterogeneity in shape (Denyer & Brown, 1990; Verheijck *et al.* 1998*a*). For our experiments, we selected spindle and elongated spindle-like cells displaying regular contractions.

Recording procedures

Membrane potentials and membrane currents were recorded using the amphotericin perforated-patch technique (Horn & Marty, 1988) to prevent run down of membrane currents by dilution of intracellular components. Patch pipettes were pulled from borosilicate glass and heat polished. The pipette solution contained (mM): potassium gluconate 125, KCl 20, amphotericin 2.2 and Hepes 10 (pH was adjusted to 7.2 with KOH). The potential between pipette and bath solution was adjusted to zero before a high-resistance seal was formed. All potentials were off-line corrected for the estimated 13 mV liquid junction potential. Membrane currents and potentials were filtered on-line with a cutoff frequency of 1 kHz, and digitized by a 12-bit analog-to-digital converter (NB-MIO-16, National Instruments Co. Austin, TX, USA) with a sampling frequency of 2 kHz. Data were stored and analysed by custom software.

Current-clamp experiments

To characterize action potentials, several action potential parameters were determined: action potential duration at 20, 50 and 100 % repolarization (APD_{20}, APD_{50}, and APD_{100}, respectively), maximal diastolic potential (MDP), action potential overshoot, cycle length and maximum upstroke velocity (dV/dt_{max}). Diastolic depolarization rate (DDR) was measured over the 50 ms time interval starting at the MDP + 1 mV. MDP + 1 mV was used rather than MDP because the time at which the MDP + 1 mV was reached could be determined more reliably than the time at which the MDP was reached. Cell capacitance (C_m) was estimated from the change in slope of the membrane potential ($\Delta(dV_m/dt)$) upon 100 ms hyperpolarizing current pulses of 25 to 50 pA (ΔI_m), which were applied shortly after the action potential had reached its MDP. Cell capacitance was calculated as $C_m = \Delta I_m / (\Delta(dV_m/dt)$, and ranged between 18 and 110 pF with a mean value of 51 ± 5.8 pF (n = 40; mean ± S.E.M.).

Voltage clamp experiments

The L-type Ca^{2+} current ($I_{Ca,L}$) and the delayed rectifier current (I_K) were elicited by series of depolarizing voltage clamp steps of 500 ms duration to membrane potentials ranging from −40 to +70 mV, with 10 mV increments. Voltage steps were applied once every 2 s from a holding potential of −40 mV. We defined $I_{Ca,L}$ as inward peak current at the beginning of a depolarizing voltage clamp step (I_{peak}). I_K was defined as the quasi steady-state current at the end of the depolarizing voltage clamp steps (I_{qss}). I_{peak} and I_{qss} are largely due to $I_{Ca,L}$ and I_K, respectively, but other currents might also contribute to these currents. The hyperpolarizing-activated current (I_f) was elicited by series of hyperpolarizing voltage clamp steps of 500 ms duration to membrane potentials ranging from −40 to −100 mV, with 10 mV decrements. Voltage clamp steps were applied once every 2 s from a holding potential of −40 mV. We defined I_f as the difference between the current at the end and start of the hyperpolarizing voltage clamp step. In addition, tail currents of the delayed rectifier current and I_f were analysed. As tail currents predominantly express deactivation of a current, they are expressed relative to the current level at the holding potential, i.e. −40 mV. The Ca^{2+}-activated Cl^- outward current ($I_{Cl(Ca)}$) was elicited by a series of depolarizing voltage clamp steps of 500 ms duration to membrane potentials ranging from −40 to +70 mV, with 10 mV increments. Voltage steps were applied once every 2 s from a holding potential of −40 mV. $I_{Cl(Ca)}$ was defined as the transient outward current sensitive to 4,4′diisothiocyanato-stilbene-2,2′-disulphonic acid (DIDS; Sigma Chemical Co). DIDS was freshly prepared as a 0.5 M stock solution in DMSO (Merck) and kept in the dark. It was diluted in Tyrode solution for use at a final concentration of 0.2 mM. The action potential clamp technique, as introduced in SA node cells by Doerr *et al.* (1989), was used to determine the time course of the $I_{Cl(Ca)}$ during the pacemaking cycle. Therefore, transmembrane potentials were recorded during stable spontaneous pacemaker activity (current clamp conditions), digitized at 10 kHz, and stored. One representative action potential waveform was selected and used as the command signal in voltage clamp conditions to drive the potential in the same cell. Continuous pacemaker activity was obtained by repeatedly applying the same waveform to the cell. At least 20 consecutive waveforms were applied in order to reach stable electrical activity. The membrane currents were recorded under control conditions, in the presence of 0.2 mM DIDS and after drug washout. All currents were normalized for cell size by dividing current amplitude by C_m. Adrenoceptor stimulation was induced by application of 1 μM noradrenaline (Centrafarm. Etten-Leur, The Netherlands).

Computer simulations

We used computer simulations to investigate the role of $I_{Cl(Ca)}$ in pacemaker activity. In these simulations, the membrane potential (V_m) of a rabbit SA nodal cell was calculated from our detailed

mathematical SA node model cell (Wilders *et al.* 1991), into which we incorporated equations for $I_{Cl(Ca)}$. The formulation of $I_{Cl(Ca)}$ was based on a model study of $I_{Cl(Ca)}$ in atrial cells (Gomis-Tena & Saiz, 1999a, 1999*b*) and is simulated as a $[Ca^{2+}]_i$-dependent conductance with (V_m-dependent) outward rectification through:

$$I_{Cl(Ca)} = P_{Cl(Ca)} f_{Cl(Ca)} R_c (V_m F^2/RT) \times (([Cl^-]_o \exp(V_m F/RT) - [Cl^-]_i)/(\exp(V_m F/RT) - 1)), \quad (1)$$

where R, T and F are universal gas constant, absolute temperature and Faraday constant, respectively, and where:

$$f_{Cl(Ca)} = ([Ca^{2+}]_i/(K_m + [Ca^{2+}]_i))^{n_H}, \quad (2)$$

and

$$R_c = 1/(1 + \exp((V_m - 44.4)/17.2)), \quad (3)$$

represent the $[Ca^{2+}]_i$ dependence and V_m dependence, respectively. Since our model does not discriminate between free and bound intracellular calcium, the $[Ca^{2+}]_i$ in eqn (2) is *total* intracellular calcium concentration. According to Gomis-Tena & Saiz (1999a, *b*), the intracellular and extracellular chloride concentrations, $[Cl^-]_i$ and $[Cl^-]_o$, are set to the Lindblad *et al.* (1996) values of 30 and 132 mM, respectively.

Following the approach of Gomis-Tena & Saiz (1999a, *b*), $I_{Cl(Ca)}$ is thus the product of: (*a*) the driving force for chloride ions, described by the Goldmann-Hodgkin-Katz equation, (*b*) the $[Ca^{2+}]_i$ dependence, tentatively described by a Hill-type equation with parameters K_m and n_H, and (*c*) the V_m dependence as is demonstrated in a variety of excitable and non-excitable cells using physiological $[Cl^-]_i$ (for reviews, see Sorota, 1999; Hume *et al.* 2000). Quantitative experimental data on the $[Ca^{2+}]_i$ dependence of $I_{Cl(Ca)}$, however, are absent. In our computer simulations the binding constant K_m and exponent n_H (in eqn (2)) were set to 5 mM and 3, respectively. Using these two parameter settings, both the experimentally observed current–voltage relationship and the moment of activation during an action potential could be well fitted (see Figs 2, 6 and 7). In addition, the permeability $P_{Cl(Ca)}$ (in eqn (1)) was set on 0.33 μL s^{-1} to match the density of $I_{Cl(Ca)}$ with our own experimental data (see Figs 2 and 7). Thus some parameter values were not based on experimental data but were chosen because they allow a proper fit of our own experimental data.

For numerical integration of differential equations we applied a simple and efficient Euler scheme with a fixed time step of 5 μs. All software was compiled as a 32-bit Windows application using Compaq Visual Fortran 6.5 and run on a 667-MHz Alpha processor workstation (Microway Screamer).

Statistics

Results are expressed as means ± S.E.M.. Data on action potential characteristics were obtained from 10 consecutive action potentials and averaged. Using statistical analysis software of Microsoft® Excel 98, statistical significance was determined by one-way or two-way analysis of variance (ANOVA) combined with Student's t test for paired or unpaired observations. A probability value of $P < 0.05$ was considered significant.

RESULTS

Sensitivity of SA node cation membrane currents to DIDS

In previous studies in atrial, Purkinje and ventricular cells, $I_{Cl(Ca)}$ was defined as the current sensitive to DIDS (Zygmunt & Gibbons, 1991, 1992; Sipido *et al.* 1993). In a first series of experiments, we tested the sensitivity to 0.2 mM DIDS of the major cationic membrane currents, i.e., I_f, $I_{Ca,L}$ (defined as the inward peak current at the beginning of a voltage clamp step, I_{peak}), and I_K (defined as

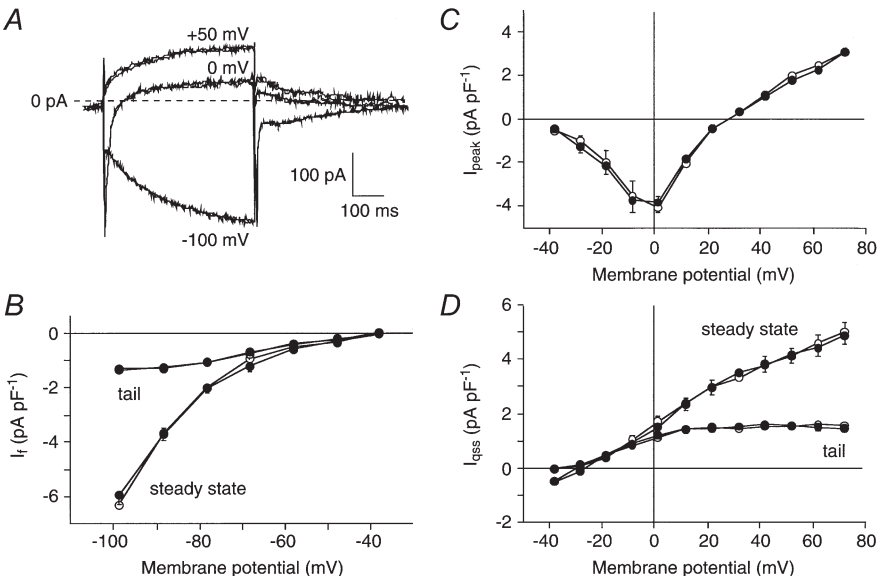

Figure 1. Effects of 0.2 mM DIDS on cationic membrane currents in sinoatrial (SA) node cells

A, superimposed current traces of an SA node cell (C_m, 57 pF) elicited by 500 ms voltage steps from −40 mV to −100, 0, and +50 mV in absence and presence of DIDS. *B–D*, average current–voltage (*I–V*) relationship of the hyperpolarization-activated current (I_f, *B*), the inward peak current at the beginning of a voltage clamp step (I_{peak}, *C*), and the quasi steady-state current at the end of a voltage clamp step (I_{qss}, *D*) in 10 cells in the absence (●) and presence (○) of DIDS. Both quasi steady-state and tail currents of I_{qss} and I_f are shown.

quasi steady-state current at the end of a voltage clamp step, I_{qss}) in SA node cells. For Fig. 1, to avoid interference with the DIDS-sensitive $I_{Cl(Ca)}$, we only used cells lacking $I_{Cl(Ca)}$ (see below). Figure 1*A* shows current traces in the absence and presence of DIDS recorded upon voltage clamp steps to −100, 0 and +50 mV, from a holding potential of −40 mV. Figure 1, *B–D*, shows the average *I–V* relationship of I_f, I_{peak}, and I_{qss} of 10 SA node cells in the absence (●) and presence (○) of 0.2 mM DIDS. Current traces as well as the *I–V* relationships before and during the administration of 0.2 mM DIDS almost completely overlap. Therefore we conclude that DIDS does not significantly affect I_f, I_{peak} (predominantly reflecting $I_{Ca,L}$), or I_{qss} (predominantly reflecting I_K).

Table 1. Action potential characteristics of SA node cells with and without $I_{Cl(Ca)}$

	No $I_{Cl(Ca)}$ (n = 14)	With $I_{Cl(Ca)}$ (n = 7)
APD_{20} (ms)	63 ± 11	70 ± 7
APD_{50} (ms)	92 ± 12	102 ± 10
APD_{100} (ms)	167 ± 17	171 ± 18
MDP (mV)	−61.0 ± 1.6	−60.4 ± 3.2
DDR (mV s^{-1})	92 ± 12	91 ± 18
Overshoot (mV)	23.3 ± 1.6	20.9 ± 2.9
dV/dt_{max} (V s^{-1})	5.9 ± 1.3	5.1 ± 1.5
Cycle length (ms)	316 ± 31	314 ± 38
Capacitance (pF)	49 ± 6	47 ± 10

Data are means ± S.E.M. APD_{20}, APD_{50} and APD_{100}, action potential duration at 20, 50 and 100% repolarization, respectively. MDP, maximal diastolic potential; DDR, diastolic depolarization rate; Overshoot, action potential overshoot and dV/dt_{max}, maximum upstroke velocity.

Presence of $I_{Cl(Ca)}$ in SA node cells

In a second series of experiments, we tested the presence of $I_{Cl(Ca)}$ in 21 single SA node cells. We applied a series of depolarizing voltage clamp steps from a holding potential of −40 mV to membrane potentials ranging from −40 to +70 mV in the absence and presence of 0.2 mM DIDS and recorded the resulting family of currents. Figure 2*A* shows two current traces elicited upon stepping to +10 mV recorded before (●) and during (○) the administration of 0.2 mM DIDS. Before administration, I_{peak} was accompanied by a transient outwardly directed current component (see arrow), which was blocked during the administration of DIDS. By digitally subtracting the two current traces, the DIDS-sensitive $I_{Cl(Ca)}$ current was obtained (Fig. 2*B*). In 7 out of 21 cells, we observed such a DIDS-sensitive current. Figure 2*C* shows the current traces of this DIDS-sensitive current recorded between −40 and +70 mV with 10 mV increments on an expanded time scale. The current is transient and outwardly directed, with characteristics similar to those of $I_{Cl(Ca)}$ in atrial, Purkinje and ventricular cells (for reviews, see Sorota, 1999; Hume *et al.* 2000). Figure 2*D* shows the average *I–V* relationship of $I_{Cl(Ca)}$

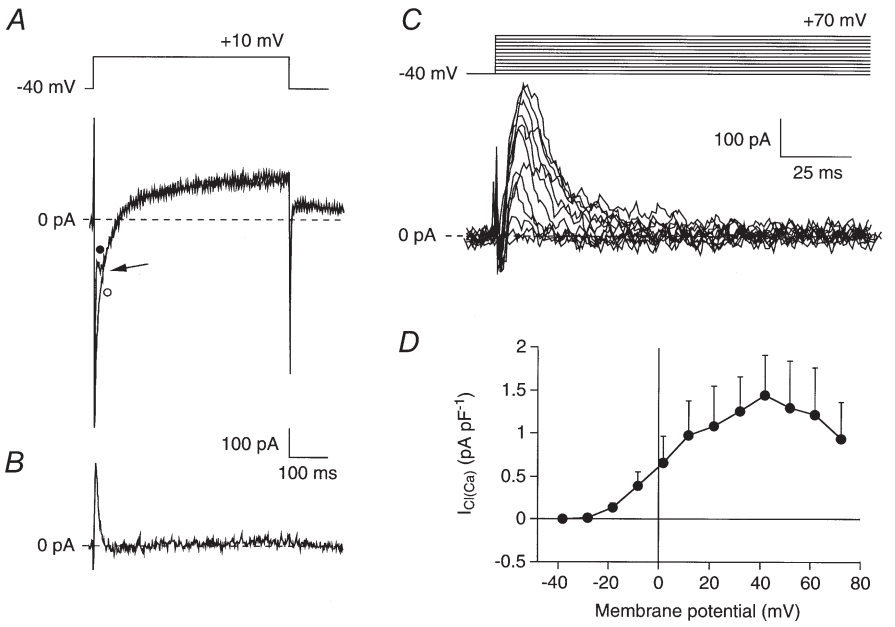

Figure 2. Presence of the Ca^{2+}-activated Cl^- current ($I_{Cl(Ca)}$) in SA node cells

A, superimposed current traces of an SA node cell (C_m, 110 pF) elicited by voltage steps from −40 to +10 mV in absence (●) and presence (○) of 0.2 mM DIDS. Arrow indicates an outwardly directed transient current, which is superimposed on the inward peak current. This transient current is blocked by DIDS. *B*, DIDS-sensitive $I_{Cl(Ca)}$ current obtained by digital subtraction of the two current traces of panel *A*. *C*, $I_{Cl(Ca)}$ measured as the DIDS-sensitive current at potentials between −40 and +70 mV in the same cell as shown in panels *A* and *B*. The current activates around −20 mV and the peak amplitude increases upon further depolarization to +40 mV. At more depolarized potentials, the peak amplitude of $I_{Cl(Ca)}$ decreases. *D*, average *I–V* relationship of $I_{Cl(Ca)}$ in 7 cells.

in these 7 SA node cells. The *I–V* relationship was bell shaped with an activation threshold around −20 mV and a maximum near +40 mV.

Our results demonstrate that $I_{Cl(Ca)}$ is present in one third of the cells tested. It might be argued that cells which display $I_{Cl(Ca)}$ are not nodal but atrial cells since we have previously described that atrial cells are present in the SA node region (Verheijck *et al.* 1998*a*). Figure 3*A* shows an example of the electrical activity of a cell with $I_{Cl(Ca)}$ (○) and one without $I_{Cl(Ca)}$ (●). The two cells clearly show similar electrical activity. Table 1 contrasts action potential parameters of the 7 SA node cells with $I_{Cl(Ca)}$ and the 14 SA node cells without $I_{Cl(Ca)}$. No difference in any action potential parameter could be detected between both groups of cells. However, a flattening of the top of the action potential was consistently present in cells including $I_{Cl(Ca)}$ (see Fig. 3*A*). Figs 3*B–D* shows that the average *I–V* relationships of I_f, I_{peak}, and I_{qss} of SA node cells with $I_{Cl(Ca)}$ (○) and without $I_{Cl(Ca)}$ (●) also do not differ from each other.

Effect of $I_{Cl(Ca)}$ blockade on electrical activity of SA nodal myocytes

Our voltage clamp experiments show that $I_{Cl(Ca)}$ is present in one third of the regularly beating single SA node cells of rabbit. Recently, it was demonstrated that the increase in subsarcolemmal intracellular Ca^{2+} concentration in spontaneously active cells occurred concomitantly with the late phase of diastolic depolarization (Huser *et al.* 2000; Rigg *et al.* 2000; Bogdanov *et al.* 2001). This implies that $I_{Cl(Ca)}$ may already be activated during the late phase of the diastolic depolarization and thus can play a role in regulating pacemaker activity. The selective action of DIDS on $I_{Cl(Ca)}$ enabled us to evaluate the contribution of $I_{Cl(Ca)}$ to spontaneous electrical activity.

Table 2. Effects of 0.2 mM DIDS on action potential characteristics of SA node cells expressing $I_{Cl(Ca)}$ (n = 7)

	Control	DIDS
APD_{20} (ms)	70 ± 7	73 ± 7*
APD_{50} (ms)	102 ± 10	104 ± 9
APD_{100} (ms)	171 ± 18	172 ± 19
MDP (mV)	−60.4 ± 3.2	−60.3 ± 3.5
DDR (mV s^{-1})	91 ± 18	105 ± 25
Overshoot (mV)	20.9 ± 2.9	22.8 ± 3.3*
dV/dt_{max} (V s^{-1})	5.1 ± 1.5	5.1 ± 1.4
Cycle length (ms)	314 ± 38	316 ± 43

Data are means ± S.E.M.. APD_{20}, APD_{50}, and APD_{100}, action potential duration at 20, 50, and 100 % repolarization, respectively. MDP, maximal diastolic potential; DDR, diastolic depolarization rate; Overshoot, action potential overshoot and dV/dt_{max}, maximum upstroke velocity. *$P < 0.05$.

The effects of DIDS on SA node action potentials were investigated on the 7 cells including $I_{Cl(Ca)}$. Figure 4 shows a typical example of an SA node action potential recorded in the absence (●) and presence (○) of 0.2 mM DIDS. DIDS predominantly increased the action potential overshoot and prolonged the APD_{20}. Table 2 summarizes the effect of 0.2 mM DIDS on action potential parameters. DIDS significantly increased the action potential overshoot and prolonged APD_{20}, without affecting dV/dt_{max}, DDR, MDP, APD_{50}, APD_{100} or cycle length. Thus, $I_{Cl(Ca)}$ modulates the action potential overshoot of SA node cells, but it does not play a significant role in beating rate regulation under normal conditions.

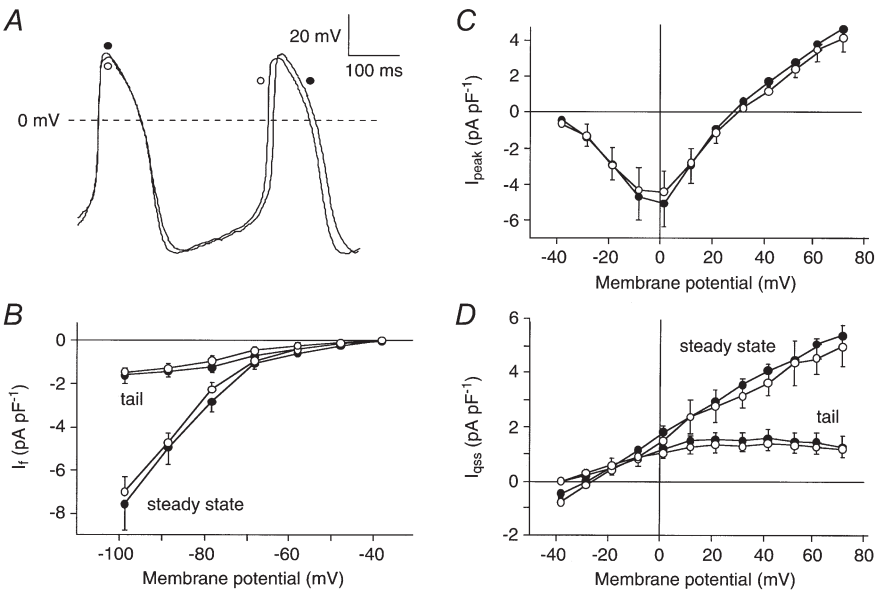

Figure 3. Electrical characteristics of SA node cells with and without $I_{Cl(Ca)}$

A, typical pacemaker activity of an SA node cell with $I_{Cl(Ca)}$ (○; C_m, 29 pF) and an SA node cell without $I_{Cl(Ca)}$ (●; C_m, 62 pF). *B–D*, average *I–V* relationship of I_f (*B*), I_{peak} (*C*), and I_{qss} (*D*) of 7 cells with (●) and 14 cells without (○) $I_{Cl(Ca)}$. Both quasi steady-state and tail currents of I_{qss} and I_f are shown.

Role of $I_{Cl(Ca)}$ on electrical activity during adrenergic stimulation

It is well known that the calcium content of the SR is increased during adrenoceptor stimulation, mainly as a consequence of an increase in $I_{Ca,L}$ (Osterrieder *et al.* 1982) and an increase in the loading of the SR (Wolska *et al.* 1996). It has been demonstrated that sympathetic stimulation with isoprenaline increased the amplitude of Ca^{2+} transient by about 75 % in guinea-pig SA node cells (Rigg *et al.* 2000) and by about 80 % in amphibian pacemaker cells (Bramich & Cousins, 1999; Ju & Allen, 1999). It is conceivable that this enhanced filling and subsequent release of Ca^{2+} from the SR during adrenergic stimulation may enhance $I_{Cl(Ca)}$ and thereby increase its role in SA node electrophysiology.

In an additional series of experiments, we determined the effect of adrenoceptor stimulation on the density of $I_{Cl(Ca)}$. Therefore, we compared the $I_{Cl(Ca)}$ already measured in the 7 cells under control conditions with $I_{Cl(Ca)}$ in another set of cells in presence of 1 μM noradrenaline. In 6 out of 16 cells, $I_{Cl(Ca)}$ was observed in the presence of noradrenaline. The percentage of cells showing $I_{Cl(Ca)}$ thus was comparable in the absence (33.3 %, $n = 21$) and presence (37.5 %, $n = 16$) of noradrenaline. This suggests that adrenoceptor stimulation could not 'wake up' $I_{Cl(Ca)}$ in cells that had no apparent current at baseline. In 5 out of these 6 cells, the voltage clamp experiments could be completed before the cells showed any signs of run down. Figure 5*A* shows the mean *I–V* relationship of $I_{Cl(Ca)}$ under control conditions (●) and in presence of noradrenaline (○). Both *I–V* relationships are bell shaped with an activation threshold around −20 mV and a peak close to +40 mV. However, density of $I_{Cl(Ca)}$ is about doubled in the presence of noradrenaline.

In the same group of cells, we measured whether $I_{Cl(Ca)}$ may influence pacemaker activity upon adrenoceptor stimulation. The effects of DIDS on SA node action potentials parameters in the presence of noradrenaline were investigated in the 6 cells expressing $I_{Cl(Ca)}$. Figure 5*B* shows a typical example of SA node action potentials recorded under control conditions (▲), in the presence of noradrenaline (●), and in the presence of noradrenaline and 0.2 mM DIDS (○). Table 3 summarizes the average action potential parameters under these three conditions. In the SA node cells expressing $I_{Cl(Ca)}$, noradrenaline induces the well-known positive chronotropic effect (for review, see Irisawa *et al.* 1993; Boyett *et al.* 2000). In addition, the cycle length and action potential overshoot were significantly decreased, while dV/dt_{max} and DDR were significantly increased. In the presence of noradrenaline, blockade of $I_{Cl(Ca)}$ with DIDS significantly increased action potential overshoot and APD_{20}, without changing the other action potential characteristics. Our experiments thus show that adrenoceptor stimulation increased $I_{Cl(Ca)}$ density and thereby enhanced its modulating role on the action potential overshoot. However, even under conditions of potentiated $I_{Cl(Ca)}$ density, this current does not play a significant role in controlling beating rate.

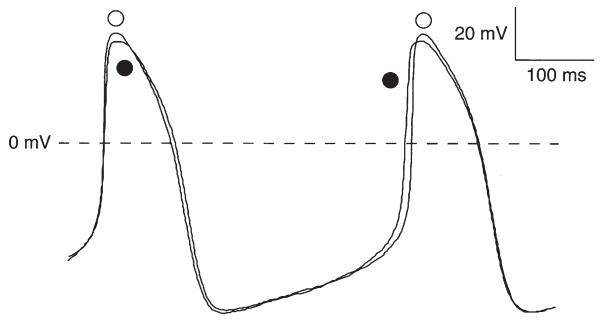

Figure 4. Effects of blockade of $I_{Cl(Ca)}$ in SA node cells

Typical pacemaker activity of a $I_{Cl(Ca)}$ expressing SA node cell (C_m, 29 pF) in absence (●) and presence (○) of 0.2 mM DIDS.

Action potential clamp and DIDS sensitive current during electrical activity

The above experiments provide evidence that $I_{Cl(Ca)}$ is active during spontaneous activity, but plays no role in regulating the intrinsic cycle length. Also, the above experiments suggest that $I_{Cl(Ca)}$ is activated late during the fast action potential depolarization. Pharmacological blockade of individual currents provides useful information,

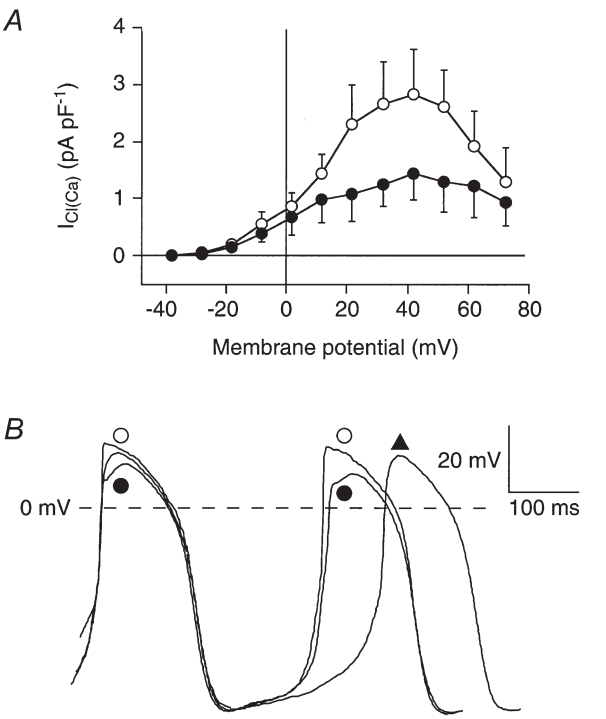

Figure 5. Adrenoceptor stimulation and $I_{Cl(Ca)}$ in SA node cells

A, average *I–V* relationship of $I_{Cl(Ca)}$ in absence ($n = 7$; ●) and presence of 1 μM noradrenaline ($n = 5$; ○). *B*, typical pacemaker activity of a $I_{Cl(Ca)}$ expressing SA node cell (C_m, 36 pF) under control conditions (▲), in the presence of 1 μM noradrenaline (●), and in the presence of both 1 μM noradrenaline and 0.2 mM DIDS (○).

Table 3. Effects of 0.2 mM DIDS on action potential characteristics of SA node cells expressing $I_{Cl(Ca)}$ (n = 6) in the presence of adrenergic receptor stimulation by 1 μM noradrenaline

	Control	Norad.	Norad. + DIDS
APD_{20} (ms)	72 ± 7	61 ± 4*	70 ± 5†
APD_{50} (ms)	105 ± 11	94 ± 7	100 ± 6
APD_{100} (ms)	160 ± 11	153 ± 5	155 ± 5
MDP (mV)	−62.0 ± 1.2	−61.4 ± 2.0	−61.6 ± 1.5
DDR (mV s^{-1})	91 ± 17	117 ± 17*	118 ± 17
Overshoot (mV)	19.3 ± 1.2	16.4 ± 1.3*	21.9 ± 1.6†
dV/dt_{max} (V s^{-1})	5.4 ± 0.6	6.8 ± 0.4*	6.6 ± 0.3
Cycle length (ms)	339 ± 16	267 ± 24*	270 ± 19

Data are means ± S.E.M. APD_{20}, APD_{50}, and APD_{100}, action potential duration at 20, 50, and 100 % repolarization, respectively. MDP, maximal diastolic potential; DDR, diastolic depolarization rate; Overshoot, action potential overshoot; and dV/dt_{max}, maximum upstroke velocity, Norad., noradrenaline. *$P < 0.05$ noradrenaline *vs.* control; †$P < 0.05$ noradrenaline + DIDS *vs.* noradrenaline.

but the changes in membrane potential induced by blockade of a single current may, in turn, affect other currents (Zaza *et al.* 1997), resulting in an overlap of primary and secondary effects of blockade, thus confusing the interpretation of results. Therefore, we carried out a final series of experiments in which we used the action potential clamp technique as introduced in SA node cells by Doerr *et al.* (1989) to avoid these problems. In these experiments, the time course of the DIDS-sensitive $I_{Cl(Ca)}$ during the pacemaking cycle is measured while clamping the membrane potential with action potential waveforms recorded from the same cell under control conditions.

Figure 6 shows a typical example of an action potential clamp experiment. Figure 6*A* shows the membrane potential recorded during stable spontaneous pacemaking activity (current clamp conditions) in a single cell under control conditions. This waveform was used as the command signal to drive the membrane potential of the same cell in the voltage clamp mode. Figure 6*B* shows the membrane current recorded under action potential clamp conditions during control conditions (upper panel), in presence of 0.2 mM DIDS (middle panel), and after wash out of the drug (lower panel). The total membrane current recorded under control conditions was close to zero (Fig. 6*B*, top), indicating that there is no difference in the intrinsic and the applied voltage waveform. The current recorded after wash out of DIDS was also close to zero, except for a short period during the action potential upstroke and shortly thereafter (Fig. 6*B*, bottom). Apparently, a difference in intrinsic and the applied voltage occurs after wash out, which is reflected by a small compensation current. The inset shows the current obtained by digitally subtracting

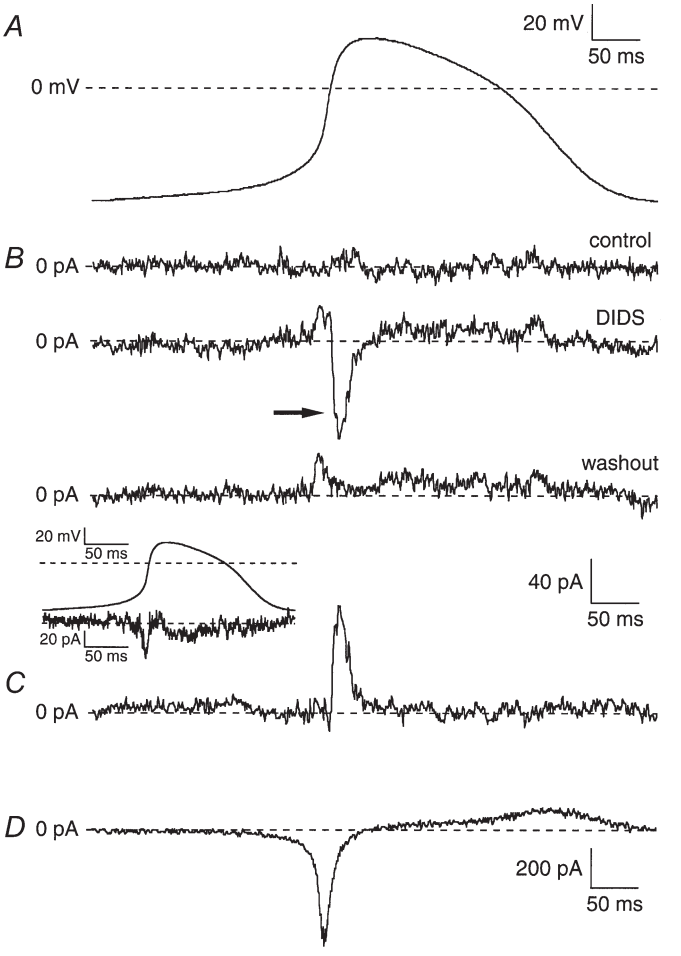

Figure 6. Action potential clamp recordings of $I_{Cl(Ca)}$ in an SA node cell

A, complete cycle of pacemaker activity of an SA node cell (C_m, 81 pF) recorded under current clamp conditions. *B*, currents recorded during reapplied pacemaker activity under voltage clamp conditions ('action potential clamp') in absence of DIDS (upper panel), in presence of 0.2 mM DIDS (middle panel), and upon wash out of the drug (lower panel). Inset shows current obtained by digitally subtracting the current trace recorded under wash out conditions from the one recorded under control conditions. *C*, DIDS-sensitive current $I_{Cl(Ca)}$ obtained by digital subtraction of compensation currents in presence and after wash out of 0.2 mM DIDS. *D*, reconstructed current (I_m) flow during the cycle of pacemaker activity. Current was calculated by $I_m = -C_m \times dV/dt$, where C_m is the membrane capacity of the cell. Note the different current scale.

the current trace recorded after wash out of DIDS from the one recorded during control conditions. The resulting current shows similarities in shape with the nifedipine-sensitive current, $I_{Ca,L}$, as recorded by Zaza and coworkers (1997) during action potential clamp conditions. The current amplitude in our experiments, however, is much smaller than reported by Zaza *et al.* (1997), suggesting that the small compensation current during the wash out conditions is due to slight run down of $I_{Ca,L}$. An additional compensation current was observed in the presence of DIDS (Fig. 6*B*, middle panel, arrow). This DIDS-induced compensation current provides a mirror image of the contribution of the blocked component, i.e. $I_{Cl(Ca)}$, to the normal pacemaking cycle. Figure 6*C* shows $I_{Cl(Ca)}$, which was obtained by digitally subtracting the current trace recorded in presence of DIDS from the one recorded after wash out of the drug. $I_{Cl(Ca)}$ measured using the action potential clamp technique is a transient outward current that becomes apparent near +5 mV and reaches a peak value of about 80 pA in the final phase of the action potential upstroke. The contribution of $I_{Cl(Ca)}$ to the current generating the action potential waveform is limited to the final phase of the upstroke and the early plateau phase. Figure 6*D* shows the reconstructed net membrane current ($I_m = -C_m dV/dt$) of the action potential shown in Panel *A*. Note that $I_{Cl(Ca)}$ is active in the phase when I_m declined from its large inward peak of about −600 pA to values near about −100 pA.

Using the action potential clamp technique, we observed $I_{Cl(Ca)}$ in 4 out of 13 (30.8 %) single SA node cells tested, which agrees with our conventional voltage clamp experiments that show that about one third of the SA node cells exhibit $I_{Cl(Ca)}$. The current was active late during the upstroke and early plateau phase. The average density of peak $I_{Cl(Ca)}$ measured during the action potential clamp measurements is 1.16 ± 0.19 pA pF^{-1} ($n = 4$), which is comparable with the current density measured during the conventional voltage clamp steps (Fig. 2*D*).

Role of $I_{Cl(Ca)}$ in pacemaker activity

Our experiments demonstrate that $I_{Cl(Ca)}$ is active late during the upstroke and early during the plateau phase of the action potential, resulting in a flattening of the top of the action potential in SA node cells. In atrial and

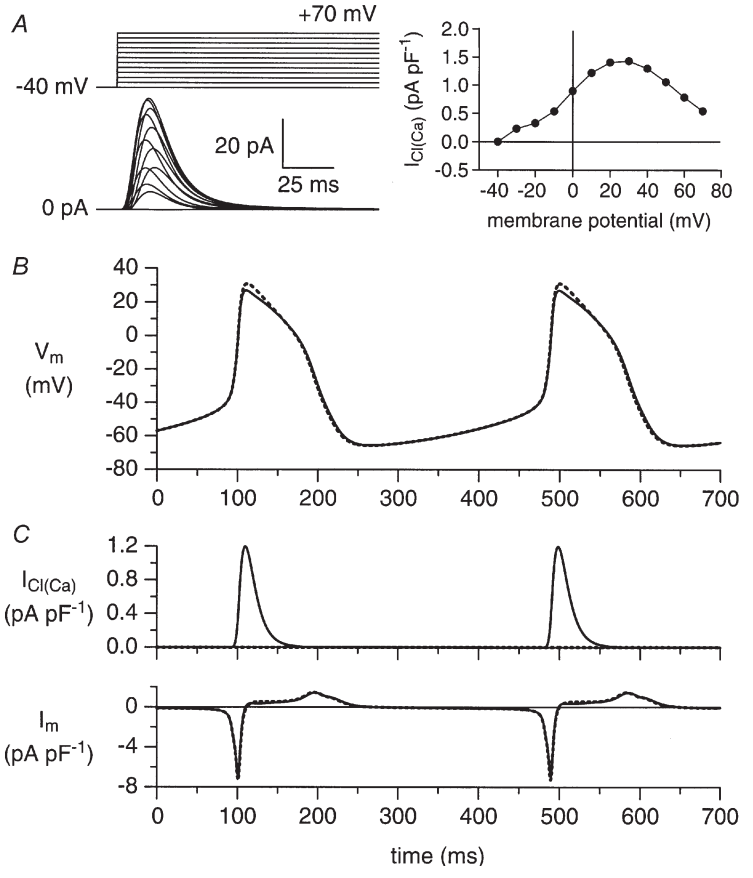

Figure 7. Computer simulations of $I_{Cl(Ca)}$ under voltage clamp and current clamp conditions

A, $I_{Cl(Ca)}$ in response to voltage clamp steps as indicated (left) and associated *I–V* relationship (right). *B*, free-running membrane potential (V_m) of the Wilders *et al.* (1991) rabbit SA nodal cell model with and without $I_{Cl(Ca)}$ (continuous and dashed lines, respectively). *C*, time course of $I_{Cl(Ca)}$ and net membrane current (I_m) during the spontaneous activity of panel *B*.

ventricular cells, it was demonstrated that such reduction of action potential overshoot has implications for action potential conduction, especially under conditions of decreased intercellular coupling (Joyner *et al.* 1996; Wang *et al.* 2000; Huelsing *et al.* 2001). As a consequence of the reduced height of the early plateau phase of the action potential, the driving force for intercellular coupling current through gap junctions was found to be reduced, thereby increasing the minimum value of intercellular coupling conductance (G_c) required for successful action potential transfer (Joyner *et al.* 1996; Wang *et al.* 2000; Huelsing *et al.* 2001). To assess the functional role of $I_{Cl(Ca)}$ in pacemaker activity, we carried out computer simulations using our previously published model of a rabbit SA node cell (Wilders *et al.* 1991), into which we incorporated the Gomis-Tena & Saiz (1999a, *b*) $I_{Cl(Ca)}$ equations which are as set out in Methods.

Validation of $I_{Cl(Ca)}$. In a first set of simulations, we validated our model description of $I_{Cl(Ca)}$ by comparing the model-generated $I_{Cl(Ca)}$ with experimental data, both under voltage clamp and current clamp conditions. Figure 7*A* (left) shows the model $I_{Cl(Ca)}$ in response to voltage clamp steps from a holding potential of–40 mV to test potentials ranging between –40 and +70 mV. We obtained current traces quite similar to those obtained with the same protocol in our experiments (Fig. 2*C*) by setting the model parameters K_m and n_H (eqn (2)) to 5 mM and 3, respectively. The model *I–V* relationship (Fig. 7*A*, right) is also quite similar to the one obtained experimentally (Fig. 2*D*). The value of the one remaining model parameter, i.e. $P_{Cl(Ca)}$ (eqn (1)), was chosen such that the maximum current density in the model *I–V* relationship (1.43 pA pF^{-1}) was similar to the average maximum density that we observed experimentally (1.44 ± 0.45 pA pF^{-1}, $n = 7$). The differences in amplitude between the current traces of Figs 2*C* and 7*A* (left) are largely due to the difference in size between the real cell (110 pF) and the model cell (32 pF).

Next, we carried out current clamp simulations with our SA nodal cell model, with the same $I_{Cl(Ca)}$ equations and parameters as used in the voltage clamp simulations, to test to which extent the results of our current clamp and action potential clamp experiments could be reproduced. Figure 7*B* shows the spontaneous activity of the model cell with and without $I_{Cl(Ca)}$ (continuous and dashed lines, respectively). Like the experimental case (Fig. 4), the most prominent effect of 'blocking' $I_{Cl(Ca)}$ is a 4 mV increase in action potential overshoot. If we increase $P_{Cl(Ca)}$ (eqn (1)) by a factor of 2, thus doubling $I_{Cl(Ca)}$, as occurs during adrenergic stimulation (Fig. 5*A*), and then study the effects of 'blocking' $I_{Cl(Ca)}$, the most prominent effect is a somewhat larger increase in action potential overshoot (7 mV), in accordance with the experimental observations (Fig. 5*B*). Figure 7*C* shows $I_{Cl(Ca)}$ and the net membrane current (I_m) during the spontaneous activity of Fig. 7*B*. The time course of those currents resembles that observed experimentally in the action potential clamp experiment of Fig. 6. Also, with a value of 1.20 pA pF^{-1}, the peak amplitude of $I_{Cl(Ca)}$ in the simulations compares well with the experimentally observed value of 1.16 ± 0.19 pA pF^{-1} ($n = 4$).

Effects of $I_{Cl(Ca)}$ on pacemaker synchronization. Subsequently, we tested the importance of $I_{Cl(Ca)}$ for pacemaker synchronization between SA node cells, which is a prerequisite for normal action potential initiation in the SA node. Previously, we demonstrated that pacemaker synchronization in pairs of SA node cells at low G_c results mainly from the phase resetting effects of the action potential of one cell on the depolarization phase of the other cell, while at higher coupling conductances, the tonic, diastolic interaction prevails (Wilders *et al.* 1996; Verheijck *et al.* 1998*b*). Consequently, we hypothesized that $I_{Cl(Ca)}$ may play a role in pacemaker synchronization under conditions of decreased intercellular coupling. To address this issue, we electrically coupled two model rabbit SA nodal cells via a variable G_c and estimated the critical value of G_c, i.e. the minimal value of G_c required for action potential synchronization. The critical G_c was determined in absence of $I_{Cl(Ca)}$ and after incorporation of $I_{Cl(Ca)}$ into the SA nodal cell model at distinct (difference in) cycle lengths. The cycle length was varied by changing the maximum conductance of I_f. As we reported previously (Wilders *et al.* 1996), critical G_c increases almost linearly with increasing difference in cycle length. The critical G_c in presence of $I_{Cl(Ca)}$, however, did not differ in any significant way from the critical G_c in absence of $I_{Cl(Ca)}$ (data not shown). Also, at higher values of G_c, $I_{Cl(Ca)}$ had minimal effects on synchronization of the model cells. These results suggest that $I_{Cl(Ca)}$ has a limited role in pacemaker synchronization.

Effects of $I_{Cl(Ca)}$ on action potential conduction. In a final set of simulations, we assessed the importance of $I_{Cl(Ca)}$ for action potential conduction between SA nodal and atrial cells. Previously, we demonstrated that our model rabbit SA nodal cell drives a real rabbit atrial cell at $G_c > 0.55$ nS (Joyner *et al.* 1998). In our simulations, we coupled the model SA node cell to a model rabbit atrial cell (Lindblad *et al.* 1996) and studied the critical G_c at which the SA node cell could successfully pace and drive the atrial cell. This critical G_c was determined in absence of $I_{Cl(Ca)}$ and after incorporation of $I_{Cl(Ca)}$ into the SA nodal cell model. The critical G_c in presence of $I_{Cl(Ca)}$ did not differ significantly from the critical G_c in absence of $I_{Cl(Ca)}$ (data not shown). Also at higher values of G_c, $I_{Cl(Ca)}$ had minimal effects on action potential transfer between the model cells. These results suggest that $I_{Cl(Ca)}$ has a limited role in action potential conduction between SA nodal and atrial cells.

DISCUSSION

In this paper we employed patch-clamp methodology and computer simulations to investigate the presence and functional role of $I_{Cl(Ca)}$ in single SA node cells of rabbit. Using the amphotericin-permeabilized patch clamp technique, we found a transient $I_{Cl(Ca)}$ in one third of the cells. The *I–V* relationship of $I_{Cl(Ca)}$ is bell shaped with an activation threshold around −20 mV, and a maximum close to +40 mV. Using the action potential clamp technique, we demonstrate that $I_{Cl(Ca)}$ is active late during the upstroke and early during the plateau phase of the action potential. Adrenoceptor stimulation with noradrenaline doubles $I_{Cl(Ca)}$, which resulted in a decrease of the action potential overshoot. Both under control conditions and upon adrenoceptor stimulation, blockade of $I_{Cl(Ca)}$ caused an increase in action potential overshoot and APD_{20}, but did not otherwise affect pacemaker activity. Our computer simulations demonstrate that $I_{Cl(Ca)}$ has a neither a role in pacemaker synchronization nor in action potential conduction.

Selective effect of DIDS on $I_{Cl(Ca)}$

In the present study, we used 0.2 mM DIDS as a tool to demonstrate the presence of $I_{Cl(Ca)}$ and to study the functional role of this current in SA node cells. DIDS, however, is not a specific blocker for the Ca^{2+}-activated Cl^- conductance, but blocks also the swelling-activated Cl^- current ($I_{Cl(swell)}$) and carriers involved in pH_i regulation, i.e. the Na^+–HCO_3^- cotransporter and the Cl^-–HCO_3^- exchanger (Leem & Vaughan-Jones, 1998; Hume *et al.* 2000).

We cannot exclude the possibility that $I_{Cl(swell)}$ also contributes to our DIDS-sensitive current, but we presume that the role of $I_{Cl(swell)}$ is limited for the following reasons. Firstly, we found a transient DIDS-sensitive current with a bell shaped *I–V* relation. These characteristics compare to those of $I_{Cl(Ca)}$ rather than to the characteristics of a swelling-activated Cl^- conductance, which is time independent and exhibits outward rectification (for review, see Vandenberg *et al.* 1996; Sorota, 1999; Hume *et al.* 2000). Secondly, the ability to observe a transient DIDS-sensitive current immediately after formation of the whole-cell perforated-patch configuration suggests that the observed current is unrelated to $I_{Cl(swell)}$, which develops over time (Vandenberg *et al.* 1996). Thirdly, $I_{Cl(swell)}$ was reported to be insensitive to β-receptor stimulation in SA node cells (Hagiwara *et al.* 1992), while in our experiments the DIDS-sensitive current was doubled in the presence of noradrenaline.

In our experiments, we expect no influences of DIDS on pH_i. We used a Hepes-buffered solution where pH_i is regulated mainly by DIDS-insensitive Na^+–H^+ exchange (Buckler *et al.* 1990; Leem & Vaughan-Jones, 1998). This is supported by the absence of changes in cycle length, while both alakalinization and acidification alter significantly the frequency of spontaneous activity in rabbit sinoatrial node (Satoh & Seyama, 1986).

Recently, it was demonstrated that DIDS (10 μM) inhibits the $I_{Ca,L}$ and I_K in colonic myocytes (Dick *et al.* 1999). We found no indications that the main cation currents in SA node cells were significantly changed by as much as 0.2 mM DIDS (Fig. 1). Our findings agree with observations made in atrial and ventricular myocytes of dog, rabbit and sheep where the drug failed to influence the $I_{Ca,L}$, the I_K, the 4-aminopyridine sensitive transient outward current, the inward rectifier current, or the action potential when $I_{Cl(Ca)}$ was already blocked by 20 mM internal EGTA (Zygmunt & Gibbons, 1992; Zygmunt, 1994; Kawano *et al.* 1995; Zygmunt *et al.* 1997; Verkerk *et al.* 2001). In addition, no effects of DIDS on $[Ca^{2+}]_i$-transients were found (Sipido *et al.* 1993; Verkerk *et al.* 2001), further indicating that Ca^{2+}-modulated membrane currents other than $I_{Cl(Ca)}$ do not play a role in the effects of the drug on action potential configuration. Thus in our experiments, the effects of DIDS on the action potentials and membrane currents seem entirely attributable to blockade of $I_{Cl(Ca)}$.

Presence of $I_{Cl(Ca)}$ in SA node cells

It has been demonstrated that SA node cells contain at least two distinct Cl^- currents. Stretch-activated anion currents were observed in single rabbit SA node cells (Hagiwara *et al.* 1992; Arai *et al.* 1996; Lei & Kohl, 1998; Kohl *et al.* 1999). Moreover, an angiotensin-II-activated chloride current was found in rabbit SA node cells suggesting that SA node cells contain protein kinase-C-sensitive Cl^- channels (Bescond *et al.* 1994). In our experiments, we additionally demonstrate that $I_{Cl(Ca)}$ is present in one third of the rabbit SA node cells (Figs 2, 5 and 6). It is unknown why $I_{Cl(Ca)}$ is non-uniformly distributed among the SA node cells. All tested cells displayed regular contractions indicating that Ca^{2+} release from the SR, and thus the substrate for activating $I_{Cl(Ca)}$, was significantly present.

The non-uniform distribution of $I_{Cl(Ca)}$ may be related to the inhomogeneity of function and structure of the SA node (for review, see Bouman & Jongsma, 1995; Boyett *et al.* 2000). Functionally, a distinction has been made in the SA node between the site of earliest activation, i.e. the primary pacemaker area, and a group of nodal fibres that are triggered to excitation, i.e. the subsidiary pacemaker area. Action potentials in the primary pacemaker area have a lower amplitude, dV/dt_{max}, MDP and a higher DDR and action potential duration compared with those in the subsidiary pacemaker area (Bouman & Jongsma, 1995; Boyett *et al.* 2000). In our study, action potential characteristics did not differ significantly between isolated SA node cells with and without $I_{Cl(Ca)}$ (Table 1). We therefore suggest that the role of pacemaker cell type in the non-uniform distribution of $I_{Cl(Ca)}$ is limited. Structurally,

Boyett and coworkers found a cell size-dependent variation in densities of various cation currents in isolated SA node cells (for review, see Boyett *et al.* 2000), although this is not a consistent finding (Wilders *et al.* 1996; Verheijck *et al.* 1998a; Wu *et al.* 2001; Mangoni & Nargeot, 2001). In the present study, we did not observe a cell size-dependent variation in density of the anion current, $I_{Cl(Ca)}$. The cell capacitance did not differ significantly between SA node cells with and without $I_{Cl(Ca)}$ (Table 1). We therefore suggest that the role of cell size in the non-uniformly distributed $I_{Cl(Ca)}$ is limited. Recently, Wu *et al.* (2001) found a morphology-dependent variation in densities of a cation current in isolated SA node cells. They observed a smaller I_f in spindle cells compared with spider-like cells. In the present study, we only used spindle-like cells. Thus, a possible role of morphological differences in the non-uniform distribution of $I_{Cl(Ca)}$ was excluded.

In our experiments, the pipette solution did not contain sodium. Sipido *et al.* (1997) and Faber & Rudy (2000) have demonstrated that this may have implications for the amplitude of Ca^{2+} transients. Sipido *et al.* (1997) performed experiments with low (0 mM) or high $[Na^+]_i$ (20 mM) and found in guinea-pig ventricular cells that Ca^{2+} transients were smaller using low $[Na^+]_i$. Comparable findings were made by Faber & Rudy (2000) using a detailed theoretical model of a guinea-pig ventricular cell. In our experiments, a lower Ca^{2+} transient may have led to a smaller current density of $I_{Cl(Ca)}$. However, we think that the absence of $[Na^+]_i$ is not responsible for the heterogeneity of presence of $I_{Cl(Ca)}$ in SA node cells. All cells showed clear contractions, and upregulation of $[Ca^{2+}]_i$ transient by 1 μM noradrenaline could not activate $I_{Cl(Ca)}$ in cells that had no apparent current at baseline. Moreover, we have used a similar pipette solution in previous studies on sheep Purkinje and ventricular cells (Verkerk *et al.* 2000, 2001), and found that $I_{Cl(Ca)}$ was present in all cells tested.

It has been suggested, based on cell size-dependent variation, that the expression of Ca^{2+}-handling proteins of the ryanodine receptor declines from the periphery to the centre of rabbit SA node cells (Musa *et al.* 1999). This suggests that intracellular Ca^{2+} regulation may vary between different parts of the SA node. In a recent report by the same group, it was found that intracellular Ca^{2+} transients as well as diastolic Ca^{2+} concentration depend on SA nodal cell size (Lancaster *et al.* 2001). It is tempting to speculate that the non-uniform distribution of $I_{Cl(Ca)}$ in SA node cells is due to heterogeneity of intracellular Ca^{2+} regulation within the SA node. Further studies are required to clarify this issue.

Functional role of $I_{Cl(Ca)}$ in SA node

Recently, it has become clear that Ca^{2+} released from the SR plays an important role in regulating pacemaker activity in mammalian SA node, probably by modulating membrane currents and exchangers (Hata *et al.* 1996; Li *et al.* 1997; Satoh, 1997; Rigg *et al.* 2000; Bogdanov *et al.* 2001). In the present study, our action potential clamp measurements demonstrate that Ca^{2+}-activated Cl^- current only is present late during the upstroke of the action potential and early during the plateau phase (Fig. 6). Both this transient nature of the current and its time of occurrence during the pacemaker cycle suggest that $I_{Cl(Ca)}$ plays a role in modulation of the action potential overshoot. This hypothesis was supported by the finding that blockade of the current increased the action potential overshoot and APD_{20} significantly (Fig. 4, Table 2), which agrees with findings in atrial and ventricular cells (Wang *et al.* 1995; Hiraoka & Kawano, 1989; Kawano & Hiraoka, 1991). We found that the modulating role of $I_{Cl(Ca)}$ on the action potential overshoot was increased during adrenoceptor stimulation (Fig. 5*B*, Table 3), most likely due to the potentiated $I_{Cl(Ca)}$ (Fig. 5*A*). In dog, rabbit and sheep ventricular cells, $I_{Cl(Ca)}$ also increases during adrenoceptor stimulation (Tseng & Hoffmann 1989; Zygmunt & Gibbons, 1991; Verkerk *et al.* 2001) and it was demonstrated that such potentiation prevents drastic action potential prolongation (Verkerk *et al.* 2001). In our experiments, however, blockade of $I_{Cl(Ca)}$ failed to significantly affect APD_{50} or APD_{100}, both under control conditions and upon adrenoceptor stimulation (Figs 4 and 5, Tables 2 and 3). Nor did we observe significant effects of $I_{Cl(Ca)}$ blockade on dV/dt_{max}, cycle length, and DDR under control conditions and adrenoceptor stimulation (Figs. 4 and 5, Tables 2 and 3). Our experiments thus in addition, show that even under conditions of enhanced $I_{Cl(Ca)}$ density, this current does not play a significant role in controlling beating rate in single SA node cells.

In our study, DIDS caused a flattening of the top of the SA node action potential, which is more pronounced during adrenoceptor stimulation (Figs 4 and 5, Tables 2 and 3). In atrial and ventricular cells, it was demonstrated that such reduction of action potential overshoot has implications for action potential conduction, especially under conditions of decreased cellular coupling (Joyner *et al.* 1996; Wang *et al.* 2000; Huelsing *et al.* 2001). Our computer simulations, however, neither revealed an important role of $I_{Cl(Ca)}$ in pacemaker synchronization of SA node cells nor in action potential transfer between SA node and atrial cells.

Conclusions

We found an $I_{Cl(Ca)}$ in single SA node cells which modulates importantly the action potential overshoot. However, we did not find a clear physiological importance of $I_{Cl(Ca)}$ for the generation or conduction of the SA nodal action potential.

REFERENCES

Arai, A., Kodama, I. & Toyama, J. (1996). Roles of Cl^- channels and Ca^{2+} mobilization in stretch-induced increase of SA node pacemaker activity. *American Journal of Physiology* **270**, H1726–1735.

Bescond, J., Bois, P., Petit-Jacques, J. & Lenfant, J. (1994). Characterization of an angiotensin-II-activated chloride current in rabbit sino-atrial cells. *Journal of Membrane Biology* **140**, 153–161.

Bogdanov, K. Y., Vinogradova, T. M. & Lakatta, E. (2001). Sinoatrial nodal cell ryanodine receptor and Na^+- Ca^{2+} exchanger. *Circulation Research* **88**, 1254–1258.

Bouman, L. N. & Jongsma, H. J. (1995). The sino-atrial node: structure, inhomogeneity and intercellular interaction. In *Pacemaker Activity and Intercellular Communication*, ed. Huizinga, J. D., pp. 37–49. CRC Press, Inc., Florida, USA.

Boyett, M. R., Honjo, M. & Kodama, I. (2000). The sinoatrial node, a heterogeneous pacemaker structure. *Cardiovascular Research* **47**, 658–687.

Bramich, N. J. & Cousins, H. M. (1999). Effects of sympathetic nerve stimulation on membrane potential, $[Ca^{2+}]_i$, and force in toad sinus venosus node. *American Journal of Physiology* **276**, H115–128.

Buckler, K. J., Denyer, J. C., Vaughan-Jones, R. D. & Brown, H. F. (1990). Intracellular pH regulation in rabbit isolated sino-atrial node cells. *Journal of Physiology* **426*P***, 22–22*P*.

Denyer, J. C. & Brown, H. F. (1990). Rabbit sino-atrial node cells: isolation and electrophysiological properties. *Journal of Physiology* **428**, 405–424.

Dick, G. M., Kong, I. D. & Sanders, K. M. (1999). Effects of anion channel antagonists in canine colonic myocytes: comparative pharmacology of Cl^-, Ca^{2+} and K^+ currents. *British Journal of Pharmacology* **127**, 1819–1831.

Doerr, T., Denger, R. & Trautwein, W. (1989). Calcium currents in single SA nodal cells of the rabbit heart studied with action potential clamp. *Pflügers Archiv* **413**, 599–603.

Faber, G. M. & Rudy, Y. (2000). Action potential and contractility changes in $[Na^+]_i$ overloaded cardiac myocytes: a simulation study. *Biophysical Journal* **78**, 2392–2404.

Gomis-Tena, J. & Saiz, J. (1999*a*). Role of Ca-activated Cl currents in the heart: a computer model. In *Computers in Cardiology,* vol. 26 pp. 109–112. IEEE Computer Society.

Gomis-Tena, J. & Saiz, F. J. (1999*b*). Role of calcium-activated chloride currents in heart in patological conditions: a computer model. In *Proceedings of the First Joint BMES/EMBS Conference*. pp. 143. IEEE Engineering in Medicine and Biology Society.

Hagiwara, N., Masuda, H., Shoda M. & Irisawa, H. (1992). Stretch-activated anion currents of rabbit cardiac myocytes. *Journal of Physiology* **456**, 285–302.

Hata, T., Noda, T., Nishimura, M. & Watanabe, Y. (1996). The role of Ca^{2+} release from the sarcoplasmic reticulum in the regulation of the sinoatrial node automaticity. *Heart and Vessels* **11**, 234–241.

Hiraoka, M. & Kawano, S. (1989). Calcium-sensitive and insensitive transient outward currents in rabbit ventricular myocytes. *Journal of Physiology* **410**, 187–212.

Horn, M. & Marty, H. (1988). Muscarinic activation of ionic currents measured by a new whole-cell recording method. *Journal of General Physiology* **92**, 145–159.

Huelsing, D. J., Pollard, A. E. & Spitzer, K. W. (2001). Transient outward current modulates discontinuous conduction in rabbit ventricular cell pairs. *Cardiovascular Research* **49**, 779–789.

Hume, J. R., Duan, D., Collier, M. L., Yamazaki, J. & Horowitz, B. (2000). Anion transport in heart. *Physiological Reviews* **80**, 31–81.

Huser, J., Blatter, L. A. & Lipsius, S. L. (2000). Intracellular Ca^{2+} release contributes to automaticity in cat atrial pacemaker cells. *Journal of Physiology* **524**, 415–422.

Irisawa, H., Brown, H. F. & Giles, W. (1993). Cardiac pacemaking in the sinoatrial node. *Physiological Reviews* **73**, 197–227.

Joyner, R. W., Kumar, R., Golod, D. A., Wilders, R., Jongsma, H. J., Verheijck, E. E., Bouman, L. N., Goolsby, W. N. & van Ginneken, A. C. G. (1998). Electrical interactions between a rabbit atrial cell and a nodal cell model. *American Journal of Physiology* **274**, H2152–2162.

Joyner, R. W., Kumar, R., Wilders, R., Jongsma, H. J., Verheijck, E. E., Golod, D. A., van Ginneken, A. C. G., Wagner, M. B. & Goolsby, W. N. (1996). Modulating L-type calcium current affects discontinuous cardiac action potential conduction. *Biophysical Journal* **71**, 237–245.

Ju, Y-K. & Allen, D. G. (1999). How does beta-adrenergic stimulation increase the heart rate? The role of intracellular Ca^{2+} release in amphibian pacemaker cells. *Journal of Physiology* **516**, 793–804.

Ju, Y-K. & Allen, D. G. (2000). The mechanisms of sarcoplasmic reticulum Ca^{2+} release in toad pacemaker cells. *Journal of Physiology* **525**, 695–705.

Kawano, S. & Hiraoka, M. (1991). Transient outward currents and action potential alternations in rabbit ventricular myocytes. *Journal of Molecular and Cellular Cardiology* **23**, 681–693.

Kawano, S., Hirayama, Y. & Hiraoka, M. (1995). Activation mechanisms of Ca^{2+}-sensitive transient outward current in rabbit ventricular myocytes. *Journal of Physiology* **486**, 593–604.

Kohl, P., Hunter, P. & Noble, D. (1999). Stretch-induced changes in heart rate and rhythm: clinical observations, experiments and mathematical models. *Progress in Biophysics and Molecular Biology* **71**, 91–138.

Lancaster, M. K., Jones, S. A., Harrison, S. M. & Boyett, M. R. (2001). Differences in the intracellular Ca^{2+} transient within the rabbit sinoatrial node. *Journal of Physiology* **533.P**, 30–30*P*.

Leem, C-H. & Vaughan-Jones, R. D. (1998). Sarcolemmal mechanisms for pH_i recovery from alkalosis in the guinea-pig ventricular myocyte. *Journal of Physiology* **509**, 487–496.

Lei, M. & Kohl, P. (1998). Swelling-induced decrease in spontaneous pacemaker activity of rabbit isolated sino-atrial node cells. *Acta Physiologica Scandinavica* **164**, 1–12.

Li, J., Qu, J. & Nathan, R. D. (1997). Ionic basis of ryanodine's negative chronotropic effect on pacemaker cells isolated from the sinoatrial node. *American Journal of Physiology* **273**, H2481–2489.

Lindblad, D. S., Murphey, C. R., Clark, J. W. & Giles, W. R. (1996). A model of the action potential and underlying membrane currents in a rabbit atrial cell. *American Journal of Physiology* **271**, H1666–1696.

Mangoni, M. E. & Nargeot, J. (2001). Properties of the hyperpolarization activated current (I_f) in isolated mouse sino-atrial node cells. *Cardiovascular Research* **52**, 51–64.

Masson-Pévet, M., Bleeker, W. K., Mackaay, A. J. C., Gros, D. & Bouman, L. N. (1978). Utrastructural and functional aspects of the rabbit sinoatrial node. In *The Sinus Node*, ed. Bonke, F. I. M., pp. 195–211. Martinus Nijhoff, The Hague, Boston, London.

Musa, H., Lei, M., Dobrzynski, H., Honjo, H., Henderson, Z., Kodama, I. & Boyett, M. R. (1999). Heterogeneous expression of the ryanodine receptor in the rabbit sinoatrial node. *Journal of Physiology* **521.*P***, 31–31*P*.

Osterrieder, W., Brum, G., Hescheler, J., Trautwein, W., Flockerzi, V. & Hofmann, F. (1982). Injections of subunits of cyclic AMP-dependent protein kinase into cardiac myocytes modulates Ca^{2+} current. *Nature* **298**, 576–578.

Rigg, L., Heath, B. M., Cui, Y. & Terrar, D. A. (2000). Localisation and functional significance of ryanodine receptors during β-adrenoceptor stimulation in the guinea-pig sino-atrial node. *Cardiovascular Research* **48**, 254–264.

Satoh, H. (1997). Electrophysiological actions of ryanodine on single rabbit sinoatrial nodal cells. *General Pharmacology* **28**, 31–38.

Satoh, H. & Seyama, I. (1986). On the mechanism by which changes in extracellular pH affect the electrical activity of the rabbit sino-atrial node. *Journal of Physiology* **381**, 181–191.

Sipido, K. R., Callewaert, G. & Carmeliet, E. (1993). $[Ca^{2+}]_i$ transients and $[Ca^{2+}]_i$-dependent chloride currents in single Purkinje cells from rabbit heart. *Journal of Physiology* **468**, 641–667.

Sipido, K. R., Maes, M. & Van de Werf, F. (1997). Low efficiency of Ca^{2+} entry through the Na^+–Ca^{2+} exchanger as trigger for Ca^{2+} release from the sarcoplasmic reticulum. *Circulation Research* **81**, 1034–1044.

Sorota, S. (1999). Insights into the structure, distribution and function of the cardiac chloride channels. *Cardiovascular Research* **42**, 361–376.

Tseng, G.-N. & Hoffmann, B. F. (1989). Two components of transient outward current in canine ventricular myocytes *Circulation Research* **64**, 633–647.

Vandenberg, J. I., Rees, S. A., Wright, A. R. & Powell, T. (1996). Cell swelling and ion transport pathways in cardiac myocytes. *Cardiovascular Research* **32**, 85–97.

Verheijck, E. E., van Ginneken, A. C. G., Bourier, J. & Bouman, L. N. (1995). Effects of delayed rectifier current blockade by E-4031 on impulse generation in single sinoatrial nodal myocytes of the rabbit. *Circulation Research* **76**, 607–617.

Verheijck, E. E., Wessels, A., van Ginneken, A. C. G., Bourier, J., Markman, M. W. M., Vermeulen, J. L. M., de Bakker, J. M. T., Lamers, W. H., Opthof, T. & Bouman, L. N. (1998*a*). Distribution of atrial and nodal cell within the rabbit sinoatrial node. *Circulation* **97**, 1623–1631.

Verheijck, E. E., Wilders, R., Joyner, R. W., Golod, D. A., Kumar, R., Jongsma, H. J., Bouman, L. N. & van Ginneken, A. C. G. (1998*b*). Pacemaker synchronization of electrically coupled rabbit sinoatrial node cells. *Journal of General Physiology* **111**, 95–112.

Verkerk, A. O., Schumacher, C. A., van Ginneken, A. C. G., Veldkamp, M. W. & Ravesloot, J. H. (2001). Role of Ca^{2+}-activated Cl^- current in ventricular action potentials of sheep during adrenoceptor stimulation. *Experimental Physiology* **86**, 151–159.

Verkerk, A. O., Veldkamp, M. W., Bouman, L. N. & van Ginneken, A. C. G. (2000). Calcium-activated Cl^- current contributes to delayed afterdepolarizations in single Purkinje and ventricular myocytes. *Circulation* **101**, 2639–2644.

Wang, Y. G., Wagner, M. B., Kumar, R., Goolsby, W. N. & Joyner, R. W. (2000). Fast pacing facilitates discontinuous action potential propagation between rabbit atrial cells. *American Journal of Physiology – Heart and Circulatory Physiology* **279**, H2095–2103.

Wang, Z., Fermini, B., Feng, J. & Nattel, S. (1995). Role of chloride currents in repolarizing rabbit atrial myocytes *American Journal of Physiology* **268**, H1992–2002.

Wilders, R, Jongsma, H. J. & van Ginneken, A. C. G. (1991). Pacemaker activity of the rabbit sinoatrial node: a comparison of mathematical models. *Biophysical Journal* **60**, 1202–1216.

Wilders, R, Verheijck, E. E., Kumar, R., Goolsby, W. N., van Ginneken, A. C. G., Joyner, R. W. & Jongsma, H. J. (1996). Model clamp and its application to synchronization of rabbit sinoatrial node cells. *American Journal of Physiology* **271**, H2168–2182.

Wolska, B. M., Stojanovic, M. O., Luo, W. Kranias, E. G. & Solaro, R. J. (1996). Effects of ablation of phospholamban on dynamics of cardiac myocytes contraction and intracellular Ca^{2+}. *American Journal of Physiology* **271**, C391–397.

Wu, J., Schuessler, R. B., Rodefeld, M. D., Saffitz, J. E. & Boineau, J. P. (2001). Morphological and membrane characteristics of spider and spindle cells isolated from rabbit sinus node *American Journal of Physiology – Heart and Circulatory Physiology* **280**, H1232–1240.

Zaza, A., Micheletti, A., Brioschi, A. & Rocchetti, M. (1997). Ionic currents during sustained pacemaker activity in rabbit sino-atrial myocytes. *Journal of Physiology* **505**, 667–688.

Zygmunt, A. C. (1994). Intracellular calcium activates a chloride current in canine ventricular myocytes. *American Journal of Physiology* **267**, H1984–1995.

Zygmunt, A. C. & Gibbons, W. R. (1991). Calcium-activated chloride current in rabbit ventricular myocytes. *Circulation Research* **68**, 424–437.

Zygmunt, A. C. & Gibbons, W. R. (1992). Properties of the calcium-activated chloride current in heart. *Journal of General Physiology* **99,** 391–414.

Zygmunt, A. C., Goodrow, R. J. & Weigel, C. M. (1998). I_{NaCa} and $I_{Cl(Ca)}$ contribute to isoproterenol-induced delayed after-depolarizations in midmyocardial cells. *American Journal of Physiology* **275**, H1979–1992.

Zygmunt, A. C., Robitelle, D. C. & Eddlestone, G. T. (1997). I_{to1} dictates behaviour of $I_{Cl(Ca)}$ during early repolarization of canine ventricle. *American Journal of Physiology* **273**, H1096–1106.

Acknowledgments

This work was partly supported by the Academic Medical Center, University of Amsterdam, The Netherlands, and by the Research Council for Earth and Life Sciences (ALW) with financial aid from the Netherlands Organization for Scientific Research (NWO) through grants 805-06.154 and 805-06.155.